OPEN

Citation: Cell Death and Disease (2014) 5, e1068; doi:10.1038/cddis.2014.44

www.nature.com/cddis

Negative regulation of chemokine receptor signaling and B-cell chemotaxis by p66Shc

L Patrussi[1,3], N Capitani[1,3], E Cannizzaro[1], F Finetti[1], OM Lucherini[1], PG Pelicci[2] and CT Baldari*[,1]

Shc (Src homology 2 domain containing) adaptors are ubiquitous components of the signaling pathways triggered by tyrosine kinase-coupled receptors. In lymphocytes, similar to other cell types, the p52 and p66 isoforms of ShcA/Shc participate in a self-limiting loop where p52Shc acts as a positive regulator of antigen receptor signaling by promoting Ras activation, whereas p66Shc limits this activity by competitively inhibiting p52Shc. Based on the fact that many signaling mediators are shared by antigen and chemokine receptors, including p52Shc, we have assessed the potential implication of p66Shc in the regulation of B-cell responses to chemokines, focusing on the homing receptors CXCR4 (C-X-C chemokine receptor type 4) and CXCR5 (C-X-C chemokine receptor type 5). The results identify p66Shc as a negative regulator of the chemotactic responses triggered by these receptors, including adhesion, polarization and migration. We also provide evidence that this function is dependent on the ability of p66Shc to interact with the chemokine receptors and promote the assembly of an inhibitory complex, which includes the phosphatases SHP-1 (Src homology phosphatase-1) and SHIP-1 (SH2 domain-containing inositol 5'-phosphatase-1), that results in impaired Vav-dependent reorganization of the actin cytoskeleton. This function maps to the phosphorylatable tyrosine residues in the collagen homology 1 (CH1) domain. The results identify p66Shc as a negative regulator of B-cell chemotaxis and suggest a role for this adaptor in the control of B-cell homing.
Cell Death and Disease (2014) **5,** e1068; doi:10.1038/cddis.2014.44; published online 20 February 2014
Subject Category: Immunity

Lymphocyte homeostasis and activation require their cyclic traffic through the secondary lymphoid organs (SLOs). Lymphocyte homing to SLOs, as well as their traffic therein, is regulated by receptors that respond to stromal cell-derived chemokines.[1] The principal B-cell homing receptors are CCR7 (C-C chemokine receptor type 7) and CXCR4 (C-X-C chemokine receptor type 4) that are responsible for their egress from the bloodstream and entry into the SLOs,[2] whereas B-cell traffic to the follicles is regulated by CXCR5 (C-X-C chemokine receptor type 5).[3] These receptors also assist retaining B-cells in the SLOs that is essential for B-cells to receive survival cues and become activated in the presence of antigen.[3]

Chemokine receptors orchestrate the sequential steps of lymphocyte homing, that is, arrest, polarization and transendothelial migration, both by triggering the conversion of integrins to their high-affinity conformation for their ligands on endothelial cells (ECs), which results in firm adhesion, and by promoting the cytoskeletal rearrangements required for polarization and migration.[4] Chemokine receptors are Gi-protein-coupled seven-spanning transmembrane receptors that reduce cyclic adenosine monophosphate (cAMP) production by inhibiting adenylate cyclase.[5] Src kinases participate in the Gi/cAMP-dependent pathways triggered by chemokine receptors, initiating a phoshorylation cascade that promotes both inside-out signaling to integrins and the Rho GTPase-dependent cytoskeletal rearrangements required for cell polarization and migration.[6–8] Chemokine receptors also trigger a Gi-independent, Janus kinase (JAK)-dependent pathway implicated in cell migration.[8] Hence, chemotaxis is coordinately regulated by multiple signaling pathways.

At variance with T cells, where signaling by chemokine receptors has been characterized to a significant extent,[9] our understanding of the signaling cascades triggered by homing receptors in B-cells is remarkably limited, notwithstanding the fact that some of the molecules implicated, such as spleen

[1]Department of Life Sciences, University of Siena, Siena, Italy and [2]Department of Molecular Oncology, European Institute of Oncology, Milan, Italy
*Corresponding author: CT Baldari, Department of Life Sciences, University of Siena, Via Aldo Moro 2, 53100 Siena, Italy. Tel: +39 577 234400; Fax: +39 577 234476; E-mail: baldari@unisi.it
[3]These authors contributed equally to this work.
Keywords: p66Shc; B lymphocytes; chemotaxis; survival; adhesion
Abbreviations: AgR, antigen receptor; BCR, B-cell receptor; Btk, Bruton's tyrosine kinase; cAMP, cyclic adenosine monophosphate; CCR7, C-C chemokine receptor type 7; Cdc42, cell division control protein 42 homolog; CH1, collagen homology 1; CLL, chronic lymphocytic leukemia; Csk, C-terminal Src kinase; CXCL12, C-X-C motif chemokine 12; CXCL13, C-X-C motif chemokine 13; CXCR4, C-X-C chemokine receptor type 4; CXCR5, C-X-C chemokine receptor type 5; EC, endothelial cell; FAK, focal adhesion kinase; FN, fibronectin; GFP, green fluorescent protein; IBMX, 3-isobutyl-1-methylxanthine; ICAM-1, intercellular adhesion molecule-1; JAK, Janus kinase; LFA-1, lymphocyte function-associated antigen-1; mAb, monoclonal antibody; NADPHox, nicotinamide adenine dinucleotide phosphate-oxidase; PH, pleckstrin homology; PIP_2/PIP_3, phosphatidylinositol 4,5-bisphosphate/(3,4,5)-trisphosphate; PI3-kinase, phosphatidylinositide 3-kinase; PKA, protein kinase A; PLCγ, phospholipase C, γ; PTX, pertussis toxin; Pyk2, protein tyrosine kinase 2; Rac1, Ras-related C3 botulinum toxin substrate 1; Rap1, Ras-proximate-1; ROS, reactive oxygen species; Shc, Src homology 2 domain containing; SHIP-1, SH2 domain-containing inositol 5'-phosphatase-1; SHP-1, Src homology phosphatase-1; SKAP-hom, Src kinase-associated phosphoprotein-homology; SLO, secondary lymphoid organ; SLP-76, SH2 domain-containing leukocyte protein of 76 kDa; Syk, spleen tyrosine kinase; S1P1, sphingosine-1-phosphate receptor 1; TK, tyrosine kinase; VEGF, vascular endothelial growth factor; VLA-4, very late antigen-4
Received 09.10.13; revised 20.12.13; accepted 02.1.14; Edited by G Ciliberto

tyrosine kinase (Syk), phosphatidylinositide 3-kinase (PI3-K) and Bruton's tyrosine kinase (Btk), are exploited therapeutically for the treatment of B-cell neoplasms.[10,11] In particular, the role of the adaptors that couple proximal tyrosine kinases (TKs) to downstream mediators in other B-cell signaling pathways remains largely elusive.

Shc (Src homology 2 domain containing) adaptors have been implicated in all central cellular processes, including proliferation, differentiation, survival and motility.[12] In lymphocytes, the p52 and p66 ShcA/Shc isoforms form a self-limiting loop, with p52Shc positively regulating antigen receptor (AgR) signaling and p66Shc acting as a competitive inhibitor.[12] Accordingly, mitogenic and survival responses to AgR engagement are enhanced in p66Shc$^{-/-}$ mice, resulting in autoimmunity.[13] Moreover, chronic lymphocytic leukemia (CLL) B-cells have a defect in p66Shc expression that contributes to their extended survival.[14] Based on the fact that many signaling mediators are shared by AgRs and chemokine receptors, including p52Shc,[15] here we have assessed the potential implication of p66Shc in the regulation of B-cell responses to chemokines. We show that p66Shc acts as a negative regulator of all steps of the chemotactic responses triggered by CXCR4 and CXCR5 by inhibiting Vav-dependent actin cytoskeleton reorganization and provide insight into the mechanism by which p66Shc uncouples these receptors from Vav activation.

Results

p66Shc inhibits CXCR4- and CXCR5-dependent B-cell adhesion and polarization. B-cell adhesion to ECs is regulated by the integrins lymphocyte function-associated antigen-1 (LFA-1), which interacts with intercellular adhesion molecule-1 (ICAM-1), and very late antigen-4 (VLA-4), which interacts with both VCAM-1 and the ECM component, fibronectin (FN). The role of p66Shc in B-cell adhesion was initially addressed in the p66Shc-deficient MEC B-cells,[14] stably transfected with a p66Shc-encoding construct, using empty vector-transfected cells as control. All transfectants expressed similar levels of LFA-1 and VLA-4, as well as CXCR4 and CXCR5 (Supplementary Figure S1A). Cells were plated on immobilized ICAM-1 or FN in the presence or absence of CXCL12 (C-X-C motif chemokine 12) or CXCL13 (C-X-C motif chemokine 13). The proportion of cells that had adhered after a short incubation was determined by flow cytometry. As expected, control cells underwent profound morphological changes in the presence of either chemokine, from a round to a polarized phenotype characterized by F-actin-rich protrusions (Figure 1a). p66Shc expression resulted in impaired CXCR4- and CXCR5-dependent adhesion to ICAM-1/FN (Figure 1b). Consistent with this finding, imaging of these cells showed that the punctate pattern of LFA-1, which results from integrin clustering following the high-affinity conformational shift,[16] was lost in p66Shc-expressing MEC cells (Supplementary Figure S2). Polarization was also impaired in the presence of p66Shc, as assessed by quantitating phalloidin-stained cells harboring a polarized morphology (Figures 1a and c).

Similar experiments were carried out on splenic B-cells from wild-type and p66Shc$^{-/-}$ mice. CXCL12- and CXCL13-dependent adhesion to ICAM-1/FN (Figure 1d), as well as polarization (Figure 1e), were significantly enhanced in p66Shc$^{-/-}$ B-cells compared with their wild-type counterparts, indicating that expression of p66Shc at physiological levels is sufficient to negatively regulate the B-cell responses to these chemokines. No difference was observed in the expression levels of either LFA-1/VLA-4 or CXCR4/CXCR5 between wild-type and p66Shc$^{-/-}$ B-cells (Supplementary Figure S1B). Hence, p66Shc acts as a negative regulator of the inside-out pathways that couple CXCR4/CXCR5 to integrin activation.

p66Shc inhibits CXCR4- and CXCR5-dependent B-cell chemotaxis. The implication of p66Shc in B-cell chemotaxis was addressed in transwell migration assays, using CXCL12/CXCL13 as chemoattractants. Both CXCR4- and CXCR5-dependent migration was impaired in p66Shc-expressing MEC cells compared with controls (Figure 2a). Consistent with this observation, migration of p66Shc$^{-/-}$ B-cells toward CXCL12/CXCL13 was enhanced compared with wild-type controls (Figure 2b).

The ability of p66Shc to affect chemotaxis was further assessed in B-cell pseudoemperipolesis assays that measure the ability of B-cells to migrate beneath co-cultured stromal cells.[17] Spontaneous emperipolesis was not affected by p66Shc. At variance, p66Shc-expressing MEC cells underwent CXCR4- and CXCR5-dependent pseudoemperipolesis with a lower efficiency compared with controls (Figure 2c). This defect was confirmed in co-culture experiments using a mixture of control and p66Shc-expressing MEC cells labeled with different fluorescent probes. Indeed, a smaller number of p66Shc-expressing cells underwent pseudoemperipolesis compared with controls within the same stromal cell layer (Figure 2c). Consistent with these results, pseudoemperipolesis was enhanced in p66Shc$^{-/-}$ B-cells compared with wild-type B-cells (Figure 2d). Hence, p66Shc acts as a negative regulator of CXCR4- and CXCR5-dependent B-cell migration.

p66Shc inhibits CXCR4- and CXCR5-dependent actin polymerization and Vav activation. The ability of p66Shc to affect B-cell polarization and migration in response to CXCL12/CXCL13 suggests that it may be implicated in coupling CXCR4/ CXCR5 to actin polymerization. This issue was addressed by confocal microscopy of control and p66Shc-expressing MEC cells plated on ICAM-1/FN in the presence or absence of CXCL12 or CXCL13. Cells were labeled with phalloidin to identify F-actin and anti-actin monoclonal antibody (mAb) as normalization control. Measurement of the F-actin fluorescence intensity showed that p66Shc expression resulted in a significant impairment in CXCR4- and CXCR5-dependent actin polymerization (Figure 3a; not shown for FN). Similar experiments were carried out on purified splenic wild-type and p66Shc$^{-/-}$ B-cells. A more robust actin polymerization in response to CXCL12/CXCL13 of p66Shc$^{-/-}$ B-cells plated on either ICAM-1 (Figure 3b) or FN (not shown) was observed when compared with wild-type B-cells, supporting a role for p66Shc in coupling CXCR4/CXCR5 to actin polymerization.

Actin polymerization is orchestrated by Rho GTPases.[18] Rac1 (Ras-related C3 botulinum toxin substrate 1) and Cdc42

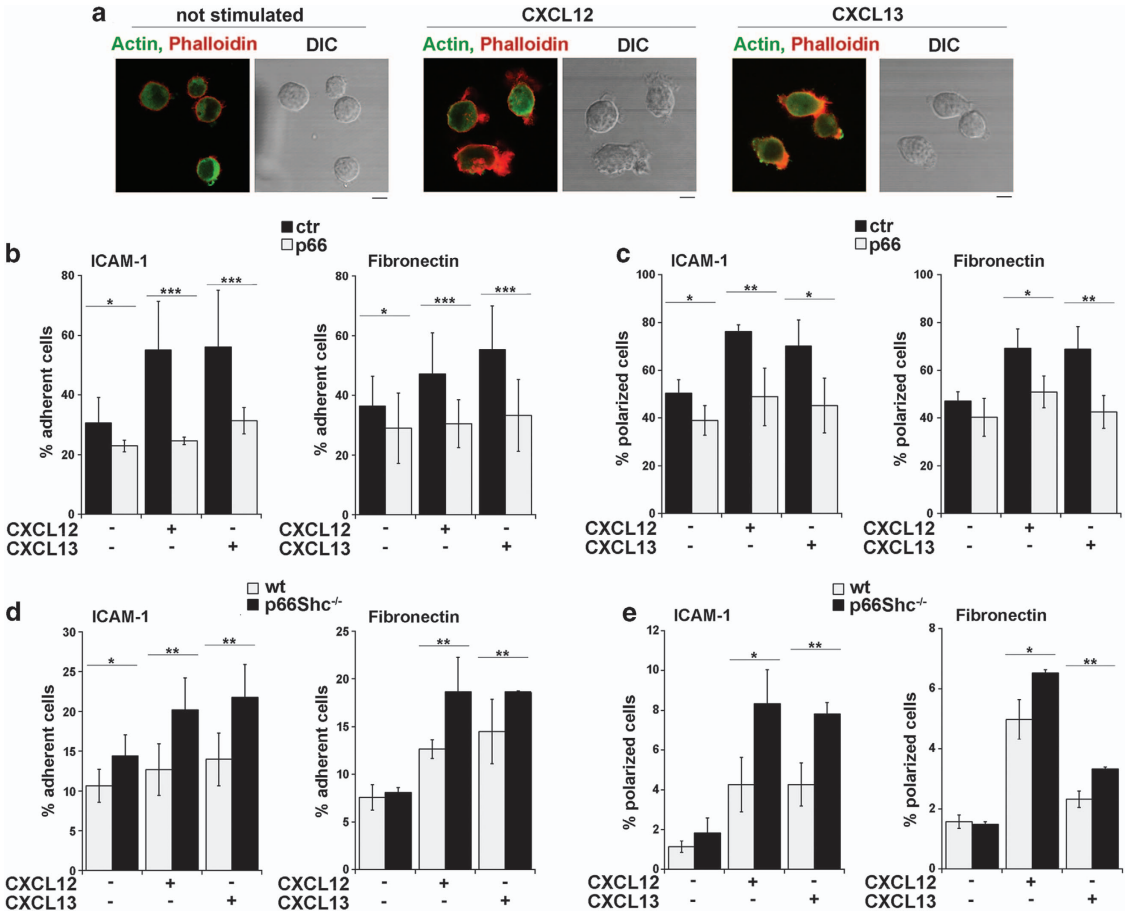

Figure 1 p66Shc inhibits CXCR4- and CXCR5-dependent, integrin-mediated B-cell adhesion and polarization. (**a**) Immunofluorescence analysis of control MEC transfectants (ctr) plated on slides coated with 10 μg/ml rhICAM-1/Fc, either unstimulated or stimulated with 100 ng/ml CXCL12 or 200 ng/ml CXCL13, and labeled with Phalloidin-TRITC (red) and anti-actin antibodies (green). Median optical sections are shown. Size bar, 5 μm. (**b**, **d**) Quantification by flow cytometry of the percentage of ctr and p66 stably transfected MEC cells (**b**) or of splenocytes from wt and p66Shc$^{-/-}$ mice (**d**) that adhered to 48-well plates coated with 10 μg/ml rhICAM-1/Fc or 10 μg/ml Fibronectin following 10 min of treatment with either 100 ng/ml CXCL12 or 200 ng/ml CXCL13. Mouse cells were labeled with anti-CD3-FITC/anti-CD22-PE antibodies before the analysis. The data, which refer to quadruplicate samples from four independent experiments, are presented as % of total input cells that remained attached to each well. Error bars, S.D. *$P \leq 0.05$; **$P \leq 0.01$; ***$P \leq 0.001$. (**c**, **e**) Quantification of the percentage of polarized cells in the ctr and p66 MEC transfectants (**c**) or in B lymphocytes purified from spleens of wt and p66Shc$^{-/-}$ mice (**e**) plated for 5 min on slides coated with either 10 μg/ml rhICAM-1/Fc or 10 μg/ml Fibronectin stimulated for 5 min with either 100 ng/ml CXCL12 or 200 ng/ml CXCL13 and labeled with Phalloidin-TRITC and anti-actin antibodies. The percentage of polarized against not-polarized cells was calculated on four different wide-field images from each well in three independent experiments. Error bars, S.D. *$P \leq 0.05$; **$P \leq 0.01$

(cell division control protein 42 homolog) activation is dependent on the guanine nucleotide exchanger, Vav, that is activated by tyrosine phosphorylation and is moreover regulated by PIP_2/PIP_3 (phosphatidylinositol 4,5-bisphosphate/(3,4,5)-trisphosphate) binding to its pleckstrin homology (PH) domain.[19] Immunoblot analysis of Vav phosphorylation in the MEC transfectants showed that p66Shc expression resulted in an impairment in CXCR4- and CXCR5-dependent Vav phosphorylation compared with controls (Figure 3c). Phospho-Vav imaging in the control transfectant revealed an enrichment of phospho-Vav in the F-actin-rich protrusions that was not detectable in the presence of p66Shc (Figure 3d). Hence, p66Shc modulates chemokine-dependent F-actin reorganization by attenuating Vav activation.

p66Shc inhibits both the Src kinase- and the PI3-K-dependent pathways triggered by CXCR4 and CXCR5. Gi-proteins promote Vav activation through two pathways activated respectively by the Gαi and the G$\beta\gamma$ subunits.[20,21] Gαi activation results in a reduction in protein kinase A (PKA) activity that reinforces the inhibitory loop controlling Src kinases by enhancing the activity of C-terminal Src kinase (Csk).[20] As a result, Lyn becomes activated and initiates a phosphorylation cascade involving Syk and Btk that together promote Vav phosphorylation.[20] G$\beta\gamma$ promotes PI3-K activation[22] that converges on Vav activation by stabilizing at the plasma membrane of both Vav and Btk through their PH domain-mediated interaction with PIP_2/PIP_3.[21]

To identify which of these pathways is regulated by p66Shc, migration assays were carried out in the presence of pharmacological inhibitors of chemokine receptor signaling. As expected, treatment of control MEC cells with pertussis toxin (PTX), a Gαi inhibitor, or the phosphodiesterase inhibitor 3-isobutyl-1-methylxanthine (IBMX), which neutralizes the effects of Gαi, resulted in a block in

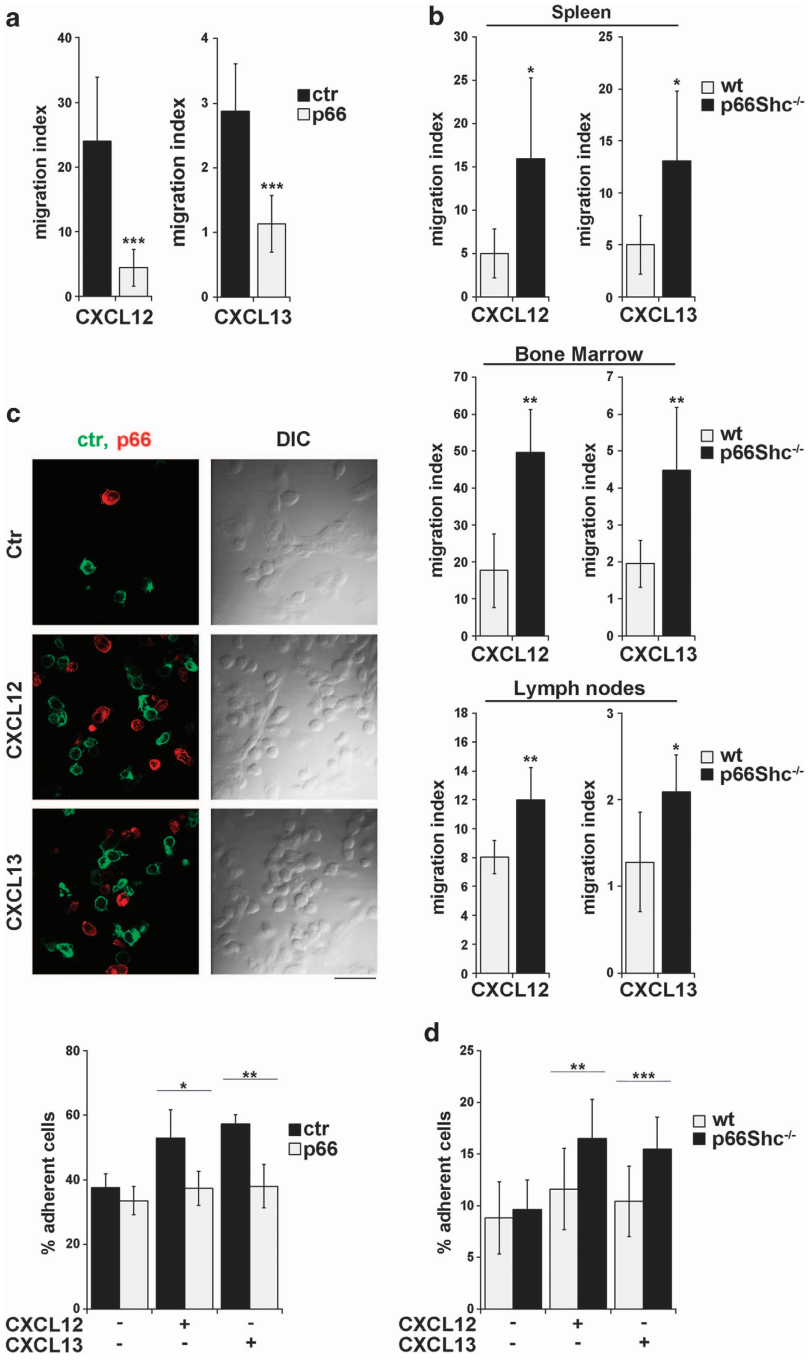

Figure 2 p66Shc inhibits CXCR4- and CXCR5-dependent B-cell chemotaxis. (**a**) Migration of ctr and p66 MEC transfectants, measured after treatment for 3 h with either 100 ng/ml CXCL12 or 200 ng/ml CXCL13. The data, obtained on duplicate samples from at least three independent experiments, are presented as mean migration index ± S.D. (ratio of migrated cells in chemokine-treated *versus* untreated samples). ***$P \leq 0.001$. An unrelated chemotactic stimulus (10 μM f-MLP) was used as a negative control. No migration of either control or p66Shc-expressing MEC cells was observed in response to this treatment (data not shown). (**b**) Migration of cells obtained from spleen, bone marrow or lymph nodes of wt and p66Shc$^{-/-}$ mice treated for 3 h with either 100 ng/ml mCXCL12 or 200 ng/ml mCXCL13 and then stained with anti-CD3-FITC/anti-CD22-PE antibodies. The data, obtained on duplicate samples from at least three independent experiments, are presented as mean migration index ± S.D. *$P \leq 0.05$; **$P \leq 0.01$. (**c** and **d**) Quantification by flow cytometry of the percentage of ctr and p66 stably transfected MEC cells (**c**, lower panel) or of splenocytes from wt and p66Shc$^{-/-}$ mice (**d**) that remained adherent to stromal cells grown on 48-well plates following stimulation with either 100 ng/ml CXCL12 or 200 ng/ml CXCL13. Before counting, MEC cells were labeled with anti-CD19-FITC mAb and mouse cells with anti-CD3-FITC/anti-CD22-PE antibodies. The data, which refer to quadruplicate samples from at least four independent experiments, are presented as % of total input cells that remained attached to each well. Error bars, S.D. *$P \leq 0.05$; **$P \leq 0.01$; ***$P \leq 0.001$. (**c**, upper panel). Immunofluorescence analysis of ctr and p66 MEC transfectants stained respectively with DiO (green) or DiI (red) incubated for 10 min on stromal cells grown on 8-well slides and either unstimulated or stimulated for 40 min with 100 ng/ml CXCL12 or 200 ng/ml CXCL13. Median optical sections are shown. Size bar, 5 μm

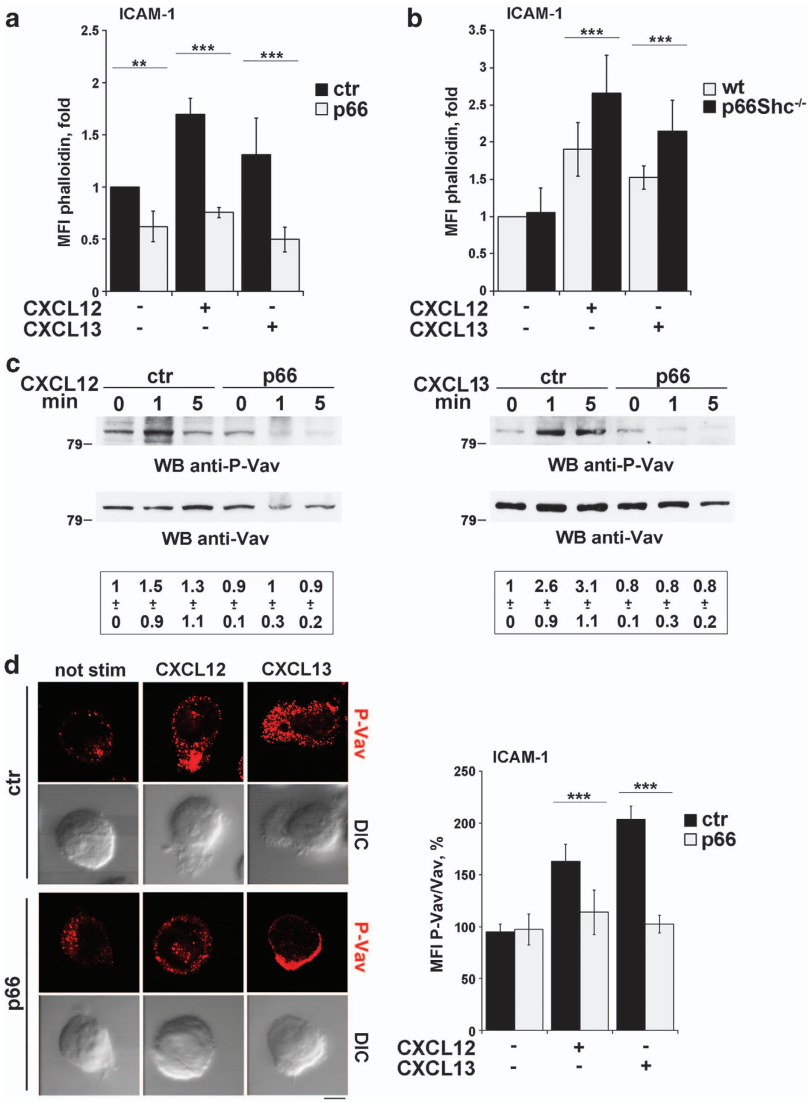

Figure 3 p66Shc inhibits CXCR4- and CXCR5-dependent actin polymerization and Vav phosphorylation. (**a** and **b**) Quantification of actin polymerization in ctr and p66 MEC transfectants (**a**) or in B lymphocytes purified from spleens of wt and p66Shc$^{-/-}$ mice (**b**), plated for 5 min on slides coated with 10 μg/ml rhICAM-1/Fc and stimulated for 5 min with either 100 ng/ml CXCL12 or 200 ng/ml CXCL13. Slides were then labeled with Phalloidin-TRITC and anti-actin antibodies. The data, calculated on four different wide-field images from four independent experiments, are presented as the mean fluorescence intensity (MFI) of Phalloidin staining in stimulated *versus* unstimulated samples, quantitated using ImageJ software and normalized to the intracellular content of actin. Error bars, S.D. $^{**}P \leq 0.01$; $^{***}P \leq 0.001$. (**c**) Immunoblot analysis with an anti-phospho-Vav antibody of postnuclear supernatants from ctr and p66 MEC transfectants either unstimulated or stimulated for 1 or 5 min with 100 ng/ml CXCL12 (left) or 200 ng/ml CXCL13 (right). Control anti-Vav immunoblots of the stripped filters are shown below. The migration of molecular mass markers is indicated. (**d**, right) Confocal microscopic analysis of Vav phosphorylation in ctr and p66 MEC transfectants plated for 5 min on slides coated with 10 μg/ml rhICAM-1/Fc and stimulated for 2 min with either 100 ng/ml CXCL12 or 200 ng/ml CXCL13. Slides were then labeled with anti-phospho-Vav and anti-Vav antibodies. Median optical sections are shown. Size bar, 5 μm. (**d**, left) Quantification of Vav phosphorylation on four different wide-field images from three independent experiments presented as the MFI of phospho-Vav staining in stimulated *versus* unstimulated samples, quantitated using ImageJ software and normalized to the intracellular content of Vav. Error bars, S.D. $^{***}P \leq 0.001$

CXCR4/CXCR5-dependent migration (Figure 4a). Migration was also inhibited by the Src kinase inhibitor PP2 and the PI3-K inhibitor wortmannin (Figure 4a), as well as the Jak inhibitor AG490 (Supplementary Figure S3). The ability of p66Shc to attenuate CXCR4- and CXCR5-dependent chemotaxis was further enhanced by PTX and IBMX, as well as by PP2 and wortmannin (Figure 4a), but not by AG490 (Supplementary Figure S3), indicating that p66Shc selectively participates in the Src and PI3-K pathways triggered by these receptors downstream of Gi activation.

To map p66Shc in the Src-dependent pathway triggered by CXCL12/CXCL13, phosphorylation of the initiating kinase Lyn and the effector kinases Syk and Btk was measured by immunoblot with phospho-specific antibodies. Lyn was activated to a similar extent by CXCR4/CXCR5 engagement in control and p66Shc-expressing MEC cells (Figure 4b). Conversely, the chemokine-dependent activation of Syk and Btk was significantly impaired in the presence of p66Shc (Figure 4b), indicating that p66Shc participates in the TK-dependent pathway triggered by CXCR4/CXCR5, attenuating signaling downstream of Lyn.

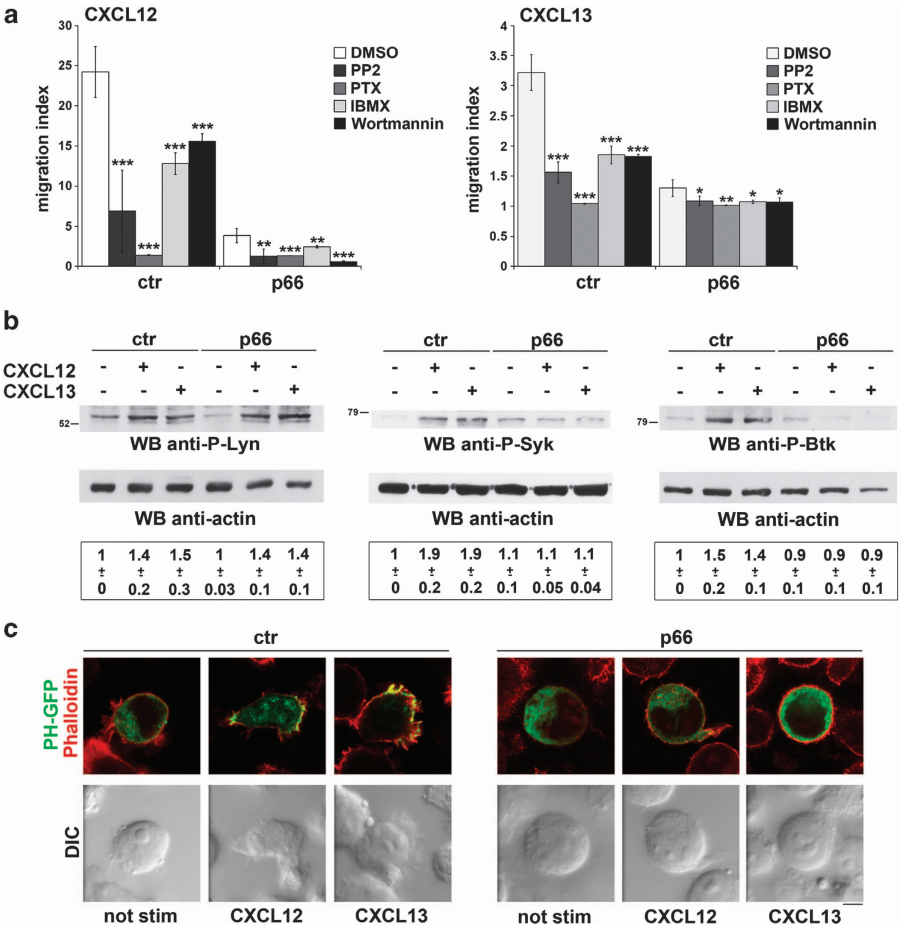

Figure 4 p66Shc inhibits both Src kinase-dependent and PI3-K-dependent signaling in response to CXCL12 and CXCL13. (**a**) Migration of ctr and p66 MEC transfectants untreated or treated for 2 h with either PP2 or 500 ng/ml PTX or 500 μM IBMX or 100 μM Wortmannin and then stimulated for 3 h with either 100 ng/ml CXCL12 (left) or 200 ng/ml CXCL13 (right). The data, obtained on duplicate samples from at least three independent experiments, are presented as mean migration index ± S.D. (ratio of migrated cells in chemokine-treated *versus* untreated samples). $^{*}P \leq 0.05$; $^{**}P \leq 0.01$; $^{***}P \leq 0.001$. (**b**) Immunoblot analysis with anti-phospho-Lyn, anti-phospho-Syk or anti-phospho-Btk antibodies of postnuclear supernatants from ctr and p66 MEC transfectants either unstimulated or stimulated for 1 min with 100 ng/ml CXCL12 or 200 ng/ml CXCL13. Control immunoblots of the stripped filters are shown below. The migration of molecular mass markers is indicated. (**c**) Immunofluorescence analysis of ctr and p66 MEC cells transiently transfected to express a PH-GFP fusion, immobilized 24 h after transfection on slides coated with 10 μg/ml rhICAM-1/Fc either unstimulated or stimulated with 100 ng/ml CXCL12 or 200 ng/ml CXCL13 and labeled with Phalloidin-TRITC (red) and anti-GFP antibodies (green). Median optical sections are shown. Size bar, 5 μm. A pharmacological CXCR4 antagonist (50 μM AMD3100, added 1 h before the chemokine) was used in combination with CXCL12 as a specificity control. No migration was observed under these conditions in either control or p66Shc-expressing MEC cells (data not shown), consistent with the suppression under these conditions of all the signaling cascades triggered by CXCR4 implicated in cell migration

The implication of p66Shc in the PI3-K pathway triggered by CXCL12/CXCL13 was also addressed, using as a readout a PI3-K reporter encoding a green fluorescent protein (GFP)-tagged PH domain. Confocal microscopy of control and p66Shc-expressing MEC cells transiently transfected with the PH-GFP construct showed that stimulation with CXCL12 or CXCL13 resulted in a plasma membrane enrichment in PH-GFP in control but not in p66Shc-expressing cells (Figure 4c). Hence, p66Shc uncouples CXCR4/CXCR5 from Vav activation by impairing both TK-dependent and phosphoinositide-dependent signaling.

Inhibition of CXCR4- and CXCR5-dependent signaling by p66Shc requires phosphorylation of its CH1 domain. The ability of p66Shc to modulate signaling depends on two activities mapping to different domains of the protein. p66Shc acts as an adaptor using the two phosphotyrosine-binding domains and the proline-rich collagen homology 1 (CH1) domain that recruits proteins through three phosphorylatable tyrosine residues (YYY239/240/317). Moreover, p66Shc has a pro-oxidant activity that maps both to a phosphorylatable serine residue in the CH2 domain (S36) and to two glutamic acid residues (EE132/133) in the cytochrome *c* binding domain.[12]

To understand whether inhibition of CXCR4/CXCR5 signaling by p66Shc depends on its adaptor or its pro-oxidant activity, we used a panel of MEC transfectants expressing point mutants of p66Shc defective for these activities. These included p66Shc3F (YYY239/240/317→FFF), p66ShcSA (S36→A) and p66ShcQQ (EE132/133→QQ). These mutants were expressed by the respective transfectants at levels comparable to the wild-type protein in p66 MEC

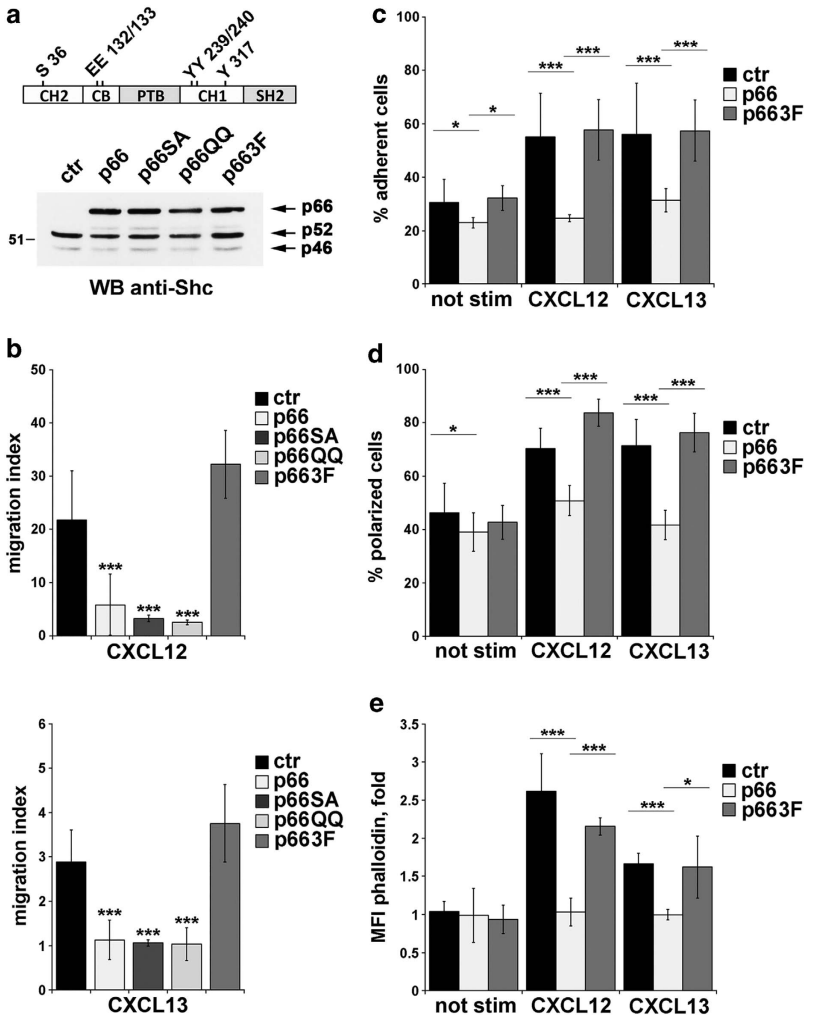

Figure 5 Inhibition of CXCR4- and CXCR5-dependent adhesion and chemotaxis by p66Shc requires tyrosine phosphorylation of its CH1 domain. (**a**) Immunoblot analysis of Shc expression in MEC B-cells stably transfected with empty vector (ctr) or an expression construct encoding either wild-type p66Shc (MEC p66) or the S36A (p66SA), EE132/133QQ (p66QQ) or YYY239/240/317FFF (p663F) mutants. A control anti-actin blot of the stripped filter is shown below. The migration of molecular mass markers is indicated. The domain structure of p66Shc showing the localization of the amino acid residues substituted in the mutants is schematized at the top of the panel. (**b**) Migration of ctr, p66, p66SA, p66QQ and p663F MEC transfectants stimulated for 3 h with either 100 ng/ml CXCL12 (upper panel) or 200 ng/ml CXCL13 (lower panel). The data, obtained on duplicate samples from at least three independent experiments, are presented as mean migration index ± S.D. (ratio of migrated cells in chemokine-treated *versus* untreated samples). $^{***}P \leq 0.001$. (**c**) Quantification by flow cytometry of the percentage of ctr, p66, and p663F cells that adhered to 48-well plates coated with 10 μg/ml rhICAM-1/Fc following treatment with either 100 ng/ml CXCL12 or 200 ng/ml CXCL13 for 10 min. The data, which refer to quadruplicate samples from four independent experiments, are presented as % of total input cells that remained attached to each well. Error bars, S.D. $^{*}P \leq 0.05$; $^{***}P \leq 0.001$. Quantification of the percentage of polarization (**d**) or actin polymerization (**e**) on ctr, p66 and p663F cells plated on slides coated with 10 μg/ml rhICAM-1/Fc, stimulated for 5 min with either 100 ng/ml CXCL12 or 200 ng/ml CXCL13 and labeled with Phalloidin-TRITC and anti-actin antibodies. The percentage of polarized cells (**d**) and the mean fluorescence intensity (MFI) of Phalloidin staining in stimulated *versus* unstimulated samples (**e**) were calculated on four different wide-field images from each well in three independent experiments. Phalloidin staining was quantitated using ImageJ software and normalized to the intracellular content of actin. Error bars, S.D. $^{*}P \leq 0.05$; $^{***}P \leq 0.001$

cells (Figure 5a). No differences were observed in the expression of LFA-1, VLA-4, CXCR4 or CXCR5 compared with control or p66Shc-expressing cells (Supplementary Figure S1A).

Expression of the reactive oxygen species (ROS)-defective mutants resulted in impaired B-cell migration and adhesion compared with control cells, similar to p66Shc (Figure 5b and Supplementary Figure S4A), ruling out a role for the pro-oxidant activity of p66Shc in this function. Conversely, the 3F mutation reversed the ability of p66Shc to inhibit B-cell chemotaxis (Figure 5b), as well as adhesion and polarization (Figures 5c and d and Supplementary Figures S4A and B). Accordingly, LFA-1 formed the typical punctate pattern resulting from integrin clustering in p66Shc3F-expressing cells (Supplementary Figure S2). The 3F mutation also fully abrogated the ability of p66Shc to inhibit CXCR4/CXCR5-dependent actin polymerization (Figure 5e and Supplementary Figure S4C), Vav phosphorylation (Figure 6a) and phospho-Vav enrichment in F-actin-rich protrusions (Figure 6b and Supplementary Figure S4D). Moreover, no defect in chemokine-dependent activation of Syk, Btk or PI3-K (Figures 6c and d) was observed in p66Shc3F-expressing

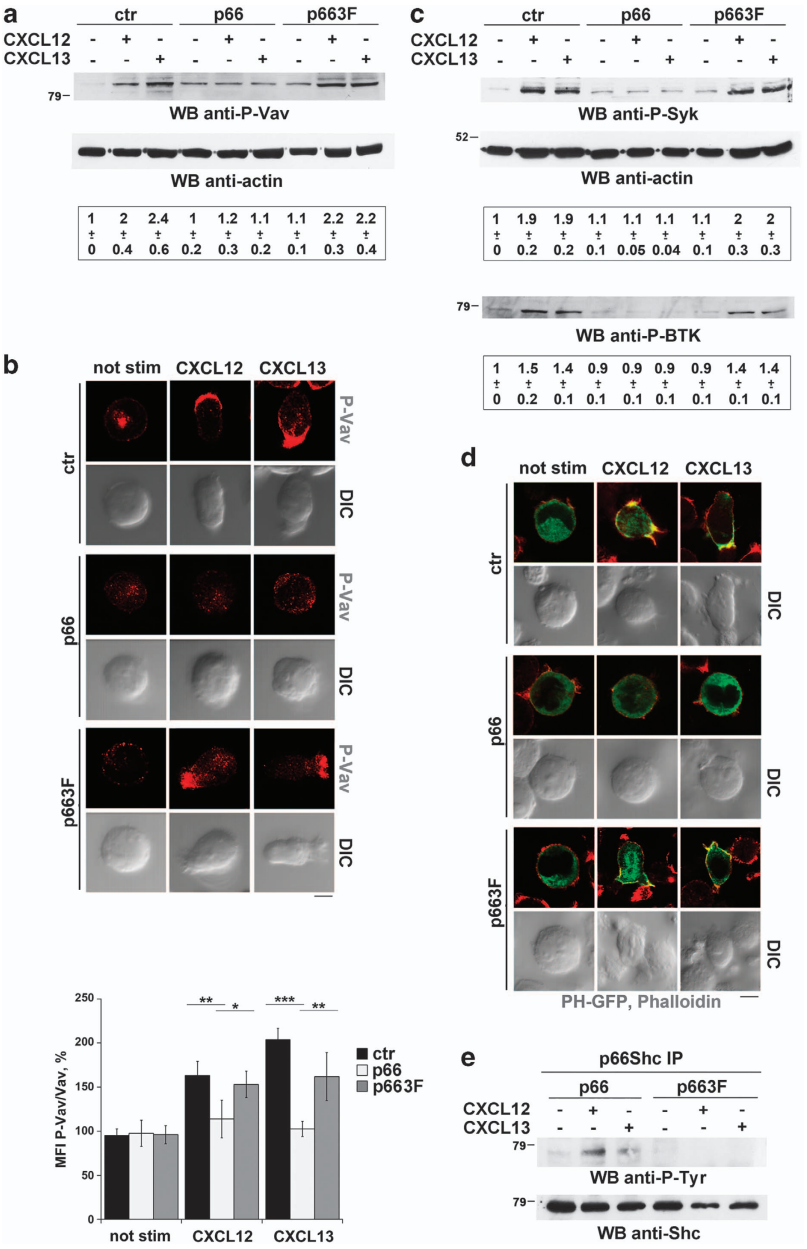

Figure 6 Inhibition of CXCR4 and CXCR5 signaling by p66Shc requires tyrosine phosphorylation of its CH1 domain. (**a**) Immunoblot analysis with anti-phospho-Vav antibody of postnuclear supernatants from ctr, p66 and p663F MEC transfectants either unstimulated or stimulated for 1 min with 100 ng/ml CXCL12 or 200 ng/ml CXCL13. A control anti-actin immunoblot of the stripped filter is shown below. The migration of molecular mass markers is indicated. (**b**, top) Confocal microscopic analysis of Vav phosphorylation in the ctr, p66 and p663F MEC transfectants plated on slides coated with 10 μg/ml rhICAM-1/Fc and stimulated for 2 min with either 100 ng/ml CXCL12 or 200 ng/ml CXCL13. Slides were then labeled with anti-phospho-Vav and anti-Vav antibodies. Median optical sections are shown. Size bar, 5 μm. (**b**, bottom) Quantification of Vav phosphorylation on four different wide-field images from three independent experiments presented as the mean fluorescence intensity (MFI) of phospho-Vav staining in stimulated *versus* unstimulated samples, quantitated using ImageJ software and normalized to the intracellular content of Vav. Error bars, S.D. $^{*}P \leq 0.05$; $^{**}P \leq 0.01$; $^{***}P \leq 0.001$. (**c**) Immunoblot analysis with anti-phospho-Syk antibody of postnuclear supernatants from ctr, p66 and p663F MEC transfectants either unstimulated or stimulated for 1 min with 100 ng/ml CXCL12 or 200 ng/ml CXCL13. A control anti-actin immunoblot of the stripped filter is shown below. The same filter was probed with anti-phospho-Btk antibody. The migration of molecular mass markers is indicated. (**d**) Immunofluorescence analysis of ctr, p66 and p663F MEC cells transiently transfected to express a PH-GFP fusion, immobilized 24 h after transfection on slides coated with 10 μg/ml rhICAM-1/Fc either unstimulated or stimulated with 100 ng/ml CXCL12 or 200 ng/ml CXCL13 and labeled with Phalloidin-TRITC (red) and anti-GFP antibodies (green). Median optical sections are shown. Size bar, 5 μm. (**e**) Immunoblot analysis with anti-phosphotyrosine antibodies of p66Shc-specific immunoprecipitates from lysates of p66 and p663F MEC cells either unstimulated or activated for 1 min with 500 ng/ml CXCL12 or 1.25 μg/ml CXCL13. The stripped filter was reprobed with anti-Shc antibodies

cells, indicating that YYY239/240/317 are required for the inhibitory effects of p66Shc on the signaling pathways that control Vav activation and actin reorganization in B-cells.

In agreement with the requirement for YYY239/240/317 phosphorylation in the regulation of CXCR4/CXCR5 signaling by p66Shc, p66Shc was found to be phosphorylated on tyrosine in response to CXCL12/CXCL13 (Figure 6e).

p66Shc recruits SHIP-1 and SHP-1 to CXCR4 and CXCR5. The results obtained with the p66Shc mutants suggests that p66Shc may interfere with CXCR4/CXCR5 coupling to Vav by acting as an adaptor to recruit negative regulators of the TK-dependent or the PI3-K-dependent pathways triggered by these receptors. To address this issue, p66Shc/p66Shc3F was immunoprecipitated from MEC transfectants expressing the GFP-tagged proteins and probed for the presence of CXCR4 and CXCR5. Both receptors were found to be engaged in a constitutive interaction with p66Shc as well as p66Shc3F (Figure 7a). Accordingly, immunofluorescence analysis showed that a proportion of p66Shc, as well as p66Shc3F, is localized at the plasma membrane under basal conditions (Figure 7b).

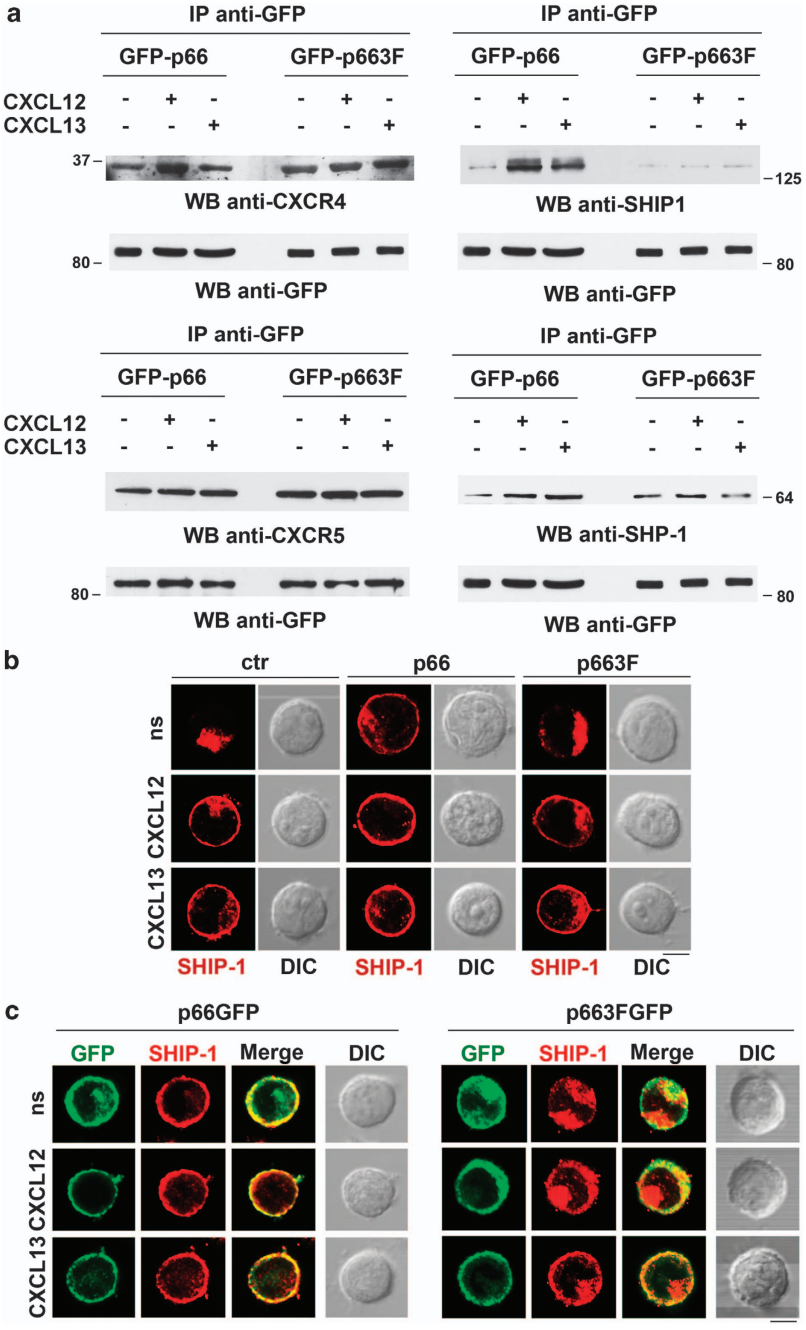

Figure 7 p66Shc recruits the phosphatases SHIP-1 and SHP-1 to CXCR4 and CXCR5. (**a**) Immunoblot analysis with anti-CXCR4, CXCR5, SHIP-1 or SHP-1 antibodies of GFP-specific immunoprecipitates from lysates of the GFP-p66 and GFP-p663F MEC transfectants either unstimulated or stimulated for 1 min with 100 ng/ml CXCL12 or 200 ng/ml CXCL13. Control anti-GFP immunoblots of the stripped filters are shown below. The migration of molecular mass markers is indicated. (**b**) Confocal microscopic analysis of SHIP-1 in the ctr, p66 and p663F MEC transfectants plated on slides coated with 10 μg/ml rhICAM-1/Fc and stimulated for 1 min with either 100 ng/ml CXCL12 or 200 ng/ml CXCL13. Slides were then labeled with anti-SHIP-1 antibody. Median optical sections are shown. Size bar, 5 μm. (**c**) Confocal microscopic analysis of GFP and SHIP-1 in the GFP-p66 and GFP-p663F MEC transfectants plated on slides coated with 10 μg/ml rhICAM-1/Fc and stimulated for 1 min with either 100 ng/ml CXCL12 or 200 ng/ml CXCL13. Slides were then labeled with anti-SHIP-1 antibody. Median optical sections are shown. Size bar, 5 μm

PIP_3 is rapidly dephosphorylated by the phosphatase SHIP-1 (SH2 domain-containing inositol 5'-phosphatase-1)[23] that negatively regulates CXCR4-dependent B-cell chemotaxis.[24] Co-immunoprecipitation experiments showed a basal SHIP-1 association with p66Shc that was strongly enhanced in response to CXCL12/CXCL13 (Figure 7a). A substantial proportion of SHIP-1 was observed at the plasma membrane under basal conditions in p66Shc-expressing MEC cells, with a significant colocalization with GFP-tagged p66Shc (Figure 7c). Although a basal association of SHIP-1 with p66Shc3F was also observed, it was not enhanced by chemokine treatment (Figure 7a). Moreover, SHIP-1 was largely cytosolic in the absence of stimulation in p66Shc3F-expressing cells, and a substantial cytosolic pool was also observed following chemokine treatment (Figure 7b). Hence, p66Shc inhibits PI-3K signaling by recruiting SHIP-1 to CXCR4/CXCR5 through its CH1 domain.

The fact that p66Shc negatively regulates the TK cascade triggered by CXCR4/CXCR5 suggests that it may counteract TKs by recruiting tyrosine phosphatases to these receptors. The tyrosine phosphatase SHP-1 (Src homology phosphatase-1) is implicated in negative signaling by a variety of receptors in hematopoietic cells.[25] Probing p66Shc-specific immunoprecipitates revealed the presence of SHP-1 under basal conditions that was enhanced in response to CXCL12/CXCL13 (Figure 7a). A basal interaction, which however did not increase in response to chemokine stimulation, was observed in cells expressing p66Shc3F (Figure 7a), indicating that p66Shc inhibition of TK signaling involves SHP-1 recruitment to CXCR4/CXCR5 through YYY239/240/Y317.

Discussion

Despite our limited mechanistic understanding of CXCR4 and CXCR5 signaling in B-cells, several signaling mediators have been identified. The integrin high-affinity conformational shift triggered by CXCR4 involves Ras-proximate-1 (Rap1), protein tyrosine kinase 2 (Pyk2) and focal adhesion kinase (FAK) activation.[26] Moreover, CXCR4 triggers the Lyn-, Syk- and PI3-K-dependent activation of Rho GTPases through a cascade involving Btk and phospholipase C, γ (PLCγ).[27] Less is known about CXCR5, although the signaling mediators identified in this pathway, such as Rap1, PI3-K and Pyk2,[27–29] suggest that it may recapitulate the CXCR4 pathway. The role of the adaptors that act as scaffolds to promote the activation and function of these molecules in the pathways triggered by AgRs has been addressed only for very few instances. Both SLP-76 (SH2 domain-containing leukocyte protein of 76 kDa), which controls TCR-dependent Rap1 activation,[30] and LAT, which couples the TCR to Vav and Rho GTPases,[31] are dispensable for CXCR4 signaling in T cells,[32,33] suggesting that different adaptors may be implicated in the assembly of the chemokine receptor-associated signalosome. However, SLP-76 has been recently identified as a common target of TCR and CXCR4 in the generation of signaling microclusters;[34] moreover, the role for SLP-76 in LFA-1-dependent T-cell adhesion has been re-evaluated in the setting of shear flow.[35] The adaptors CrkL and Cbl-b are recruited in a multimolecular complex in response to CXCR4 engagement in a pre-B lymphoma line,[36] but their role in B-cell migration has not been directly addressed. The results presented here contribute to filling this gap by identifying p66Shc, which participates as a negative regulator in B-cell receptor (BCR) signaling,[37] as a central component of the pathways that couple CXCR4/CXCR5 to integrin activation and actin dynamics in B-cells. Although the physiological levels of p66Shc expression in primary B-cells are relatively low, they are clearly sufficient to tune down the responses triggered by these receptors, as highlighted by their significant enhancement in p66Shc$^{-/-}$ B-cells.

p66Shc appears to function downstream of Gi activation at the early steps of CXCR4/CXCR5 signaling in the pathways that couple Lyn and PI3-K to Vav, but not in the Gi-independent Jak pathway, as supported by the exacerbation of the chemotaxis defects in p66Shc-expressing B-cells when treated with either PTX or PP2 or wortmannin, but not AG490. A comparison of Lyn, Syk and Btk activation in B-cells differing in p66Shc expression maps p66Shc downstream of Lyn. Lyn activation is believed to occur through its recruitment to lipid rafts with the activated chemokine receptors.[38] That p66Shc does not affect Lyn activation indicates that its constitutive interaction with CXCR4/CXCR5 does not impinge on either their raft clustering or their ability to recruit Lyn. A mechanism by which p66Shc attenuates TK signaling downstream of Lyn can be proposed based on our finding that it interacts with SHP-1 that binds to and dephosphorylates Syk in B-cells.[39] This does not rule out the possibility of a transdominant inhibition of p52Shc that participates in TCR transactivation by CXCR4 in T cells.[15] Nevertheless, this possibility appears unlikely, as this inhibitory function of p66Shc relies on S36 phosphorylation,[12] whereas the data presented here indicate that this molecular determinant is dispensable for the negative regulation of CXCR4/CXCR5 signaling by p66Shc in B-cells.

Inhibition of phosphoinositide signaling by p66Shc is likely to contribute to the Vav activation defect in response to CXCR4/CXCR5, as both Btk and Vav are provided of a phosphoinositide-binding domain.[21] The ability of p66Shc to reduce phosphoinositide accumulation may moreover contribute to the impairment of inside-out signaling to integrins by affecting the assembly of the complex that promotes Rap1 activation that in B-cells includes the PH domain-containing adaptor Src kinase-associated phosphoprotein-homology (SKAP-hom).[40] Although a modulation of PI3-K activity by p66Shc cannot be ruled out, inhibition of CXCR4/CXCR5-dependent phosphoinositide accumulation by p66Shc stems, at least in part, from its ability to enhance SHIP-1 recruitment to the plasma membrane, similar to what we have described for FcεRI signaling in mast cells.[41] SHIP-1 associates with p52Shc through a bidentate interaction involving binding of the SHIP-1 SH2 domain to phosphorylated YYY239/240/317, as well as binding of the phosphorylated SHIP-1 NPXY motif to the Shc PTB domain.[42,43] The basal association of p66Shc with CXCR4/CXCR5 suggests that p66Shc could recruit an initial SHIP-1 pool to the receptors in the absence of stimulation, as supported by the constitutive membrane localization of SHIP-1 in p66Shc-expressing cells. Following chemokine binding, CXCR4/CXCR5 could promote p66Shc and SHIP-1 phosphorylation, thereby stabilizing the p66Shc-SHIP-1 complex at the plasma membrane, as supported by the chemokine-dependent enhancement in SHIP-1 binding to p66Shc, but not p66Shc3F. It is noteworthy that SHIP-1$^{-/-}$

B-cells display adhesion and chemotaxis defects similar to the ones described here for p66Shc$^{-/-}$ B-cells,[24] supporting the notion that p66Shc negatively regulates these processes through SHIP-1.

The ability of p66Shc to generate ROS appears in contrast to its inhibitory effects on B-cell adhesion and migration, as these processes are regulated by oxidants. During EC migration, the NADPHox (nicotinamide adenine dinucleotide phosphate-oxidase) subunits NOX2 and p47^{phox} are targeted to the leading edge where they generate superoxide[44,45] that promotes cell migration through the oxidation-dependent inhibition of protein phosphatases.[46] ROS also promote leukocyte adhesion to ECs by enhancing ICAM-1 and P-selectin expression,[47,48] and by inducing a turnover of EC junction proteins.[49] p66Shc promotes ROS accumulation by both inhibiting forkhead transcription factors that control the expression of anti-oxidant enzymes[50] and interrupting the mitochondrial respiratory chain.[51] Subcellular compartmentalization of ROS generation has emerged as an important feature of ROS signaling.[52] We can hypothesize that p66Shc may generate ROS at locations that are not relevant to the signaling pathways that mediate CXCR4/CXCR5-dependent B-cell migration. In support of this notion, NADPHox inhibition did not affect the ability of p66Shc to increase intracellular ROS in T cells (A Nuccitelli and CT Baldari, unpublished). It is noteworthy that p66Shc mediates anoikis in fibroblasts by promoting RhoA activation and focal adhesion formation[53] and promotes VEGF-dependent ROS production in ECs by activating Rac1 and NAPDHox.[54] Hence, the effects of p66Shc on chemotaxis and the role of its pro-oxidant activities in this process appear to be cell type-specific.

We have recently shown that p66Shc modulates the expression of receptors that control B-cell entry (CCR7) and egress (sphingosine-1-phosphate receptor 1 (S1P1)) through its pro-oxidant activity,[14] suggesting its implication in their trafficking to SLOs. The results presented here show that p66Shc can additionally participate in B-cell homing by attenuating signaling to the actin cytoskeleton by CXCR4/CXCR5, acting as an adaptor to recruit negative regulators. Collectively, the data identify p66Shc as a multifunctional regulator of B-cell trafficking.

Materials and Methods

Cell lines, plasmids, antibodies and reagents. A panel of MEC-1 B-cell stable transfectants expressing either p66Shc (p66) or the p66ShcSA (p66SA) or p66ShcQQ (p66QQ) point mutants, as well as an empty vector transfectant (ctr), were previously described.[14] A MEC-1 transfectant was generated using a construct encoding a p66Shc point mutant lacking the three phoshorylatable tyrosine residues (YYY239/240/317) in the CH1 domain (p66Shc3F).[55] The cDNAs encoding p66Shc and p66Shc3F were cloned into pEGFP-C3 (Invitrogen, Carlsbad, CA, USA) and stably transfected into MEC-1 cells as described previously.[14] A vector encoding the GFP-tagged Akt PH domain[56] was transiently transfected into the stable control, p66 and p663F transfectants. Murine OP9[57] and human HS-5[58] stromal cells were used for pseudoemperipolesis experiments.

Phosphospecific antibodies recognizing the phosphorylated active forms of Syk, Btk and Lyn were from Cell Signaling Technology (Beverly, MA, USA) and anti-phospho-Vav was from Biosource (Camarillo, CA, USA). Anti-Erk2, anti-SHIP-1 and anti-Shc antibodies were from Santa Cruz Biotechnology (Santa Cruz, CA, USA), anti-actin was from Chemicon Int. (Temecula, CA, USA), and anti-phosphotyrosine, anti-Vav and anti-Shc antibodies were from Millipore (Billerica, MA, USA). Anti-CXCR5 and anti-SHP-1 antibodies were from Abcam (Cambridge, UK), anti-CXCR4 polyclonal antibodies were from Sigma-Aldrich (St. Louis, MO, USA), anti-CXCR4 mAbs were from Abnova (Aachen, Germany), anti-GFP polyclonal and mAbs were from Invitrogen. Anti-CXCR4 (12G5) antibodies were kindly provided by J Hoxie, Leukosite Inc. and the MRC AIDS Reagent Project (Cambridge, MA, USA). p66Shc was immunoprecipitated using a rabbit polyclonal antiserum raised against a CH2-glutathione *S*-transferase (GST) fusion protein.[59] Secondary peroxidase-labeled antibodies were from GE Healthcare (Fairfield, CT, USA). Anti-CD11a, anti-human CD3 and CD19, anti-mouse CD3 and CD22 and secondary fluorochrome-labeled antibodies were from eBioscience (San Diego, CA, USA); anti-GFP and Alexa Fluor 488- and 555-labeled secondary antibodies were from Invitrogen (Leek, The Netherlands). Human and mouse CXCL12 and CXCL13, FN, AG490, PP2, AMD3100, IBMX, f-MLP and TRITC-labeled Phalloidin were purchased from Sigma-Aldrich. PTX was purchased from Sigma-Aldrich. rhICAM-1/Fc was purchased from R&D Systems (Minneapolis, MN, USA). The chemiluminescence detection kit was from Pierce (Rockford, IL, USA). DiO and DiI fluorescent dyes were purchased from Molecular Probes (Invitrogen).

Mice. p66Shc$^{-/-}$/129 mice (p66Shc$^{-/-}$) have been previously described.[59] Analyses were performed on age- and sex-matched 2–9-month-old wild-type 129 mice (wt). All experiments were carried out in agreement with the Guiding Principles for Research Involving Animals and Human Beings and approved by the local ethics committee. Experiments were carried out on spleen, lymph nodes and bone marrow suspensions, or splenic B-cells negatively purified by immunomagnetic sorting using the Dynabeads Mouse CD43 Negative Isolation Kit (Invitrogen) ($>85\%$ purity).

Activations and immunoprecipitations. Cells were starved for 2 h in RPMI/1% BSA. Activations with CXCL12 or CXCL13 (10–500 ng/ml, 0.1–1.25 μg/ml, respectively, depending on cell concentration) were carried out at 37°C in RPMI/1% BSA. Cells were lysed in 1% Triton X-100 in 20 mM Tris-HCl, pH 8, 150 mM NaCl (in the presence of protease inhibitor cocktail, Invitrogen), resolved by SDS-PAGE and transferred to nitrocellulose (Whatman, GE Healthcare). Alternatively, postnuclear supernatants from $2.5–5 \times 10^7$ cells/sample were immunoprecipitated using the appropriate antibodies and protein A-Sepharose (GE Healthcare).

Flow cytometry and chemotaxis assay. Transwell migration assays were carried out as described previously.[15] Migrated cells were counted by flow cytometry. Mouse cells were stained with anti-CD3/anti-CD22 antibodies before analysis. The migration index was calculated by determining the ratio of migrated cells in treated *versus* untreated samples.

Adhesion assay. The 48-well plates were coated o/n at 4°C with either 10 μg/ml FN or 10 μg/ml rhICAM-1/Fc, washed with PBS and incubated for 30 min at 37°C with RPMI/1% BSA. Then, 2×10^5 cells/well serum-starved B-cells were added. The plates were incubated at 37°C for 10 min, then added with 100 ng/ml CXCL12 or 200 ng/ml CXCL13 for further 10 min. Cells that had not adhered (recovered in medium and washes) were resuspended in 0.2 ml RPMI. Cells that remained adherent after 3 washes were recovered by 1-min incubation with trypsin/EDTA, immediately added with RPMI-10% BCS, washed and resuspended in 0.2 ml RPMI. Cells were counted by flow cytometry. Mouse cells were stained with anti-CD3/CD22 antibodies before flow cytometry. The percentage of adherent cells was calculated as follows:

$$\frac{\text{no. adherent}}{\text{no. total}} \times 100$$

where 'total' is the sum of adherent and nonadherent cells/well.

Pseudoemperipolesis assay. Stromal cells were seeded on 48-well plates (1.5×10^5 cells/well) in RPMI/10% BCS and cultured to confluence. Then, 2×10^5 cells/well serum-starved B-cells were added. Plates were incubated at 37°C for 10 min, then added with 100 ng/ml CXCL12 or 200 ng/ml CXCL13 for 40 min. Wells were vigorously washed three times with RPMI and the cells that had not adhered (recovered in medium and washes) were resuspended in 0.2 ml medium. The stromal cell layer containing migrated cells was trypsinized as described above and cells were suspended in 0.2 ml medium. Cells were counted by flow cytometry. All samples were stained with anti-CD19 (human cells) or anti-CD3/CD22 (mouse cells) antibodies before flow cytometry to exclude stromal cells. The percentage of migrated cells was calculated as above.

Immunofluorescence, confocal microscopy and polarization assay. Diagnostic microscope slides were coated with FN or rhICAM-1/Fc and cells (1×10^5/sample) were allowed to adhere for 5 min before stimulation for 2–5 min with 100 ng/ml CXCL12 or 200 ng/ml CXCL13. Cells transiently transfected with the PH-GFP-expressing vector were used 24 h after transfection. Slides were immediately fixed in 4% paraformaldehyde at RT for 20 min as previously described.[60] For SHIP-1 and SHP-1 staining, cells were plated for 15 min on polylysine-coated slides and then stimulated as above. Following fixation, samples were washed 5 min in PBS and incubated with primary antibodies or TRITC-labeled Phalloidin o/n at 4°C or 1 h at RT. After washing in PBS, samples were incubated for 1 h at RT with Alexa Fluor 488- and 555-labeled secondary antibodies.

Confocal microscopy was carried out on a Zeiss LSM700 (Carl Zeiss, Jena, Germany) using a $\times 63$ objective. Images to quantify were acquired with pinholes opened to obtain 0.8 μm-thick sections. Detectors were set to detect an optimal signal below the saturation limits. Images were processed with Zen 2009 image software (Carl Zeiss) and analyses were performed using ImageJ software (downloaded from http://www.embl-heidelberg.de/eamnet/).

For the polarization assay, slides were stained with TRITC-labeled Phalloidin and anti-actin mAb, four different wide-field images/well (at least 25 cells/field) were taken and the percentage of polarized cells (with protrusions or with irregular morphology; see representative images in Figure 1a) against total cells was calculated. In the same images, mean fluorescence intensity (MFI) of Phalloidin and actin staining was quantitated using ImageJ software. For each the Phalloidin staining was normalized to the actin staining.

RNA purification and real-time PCR. Total RNA was extracted from MEC transfectants or mouse B lymphocytes and retrotranscribed as previously described.[37] Real-time PCR was performed in triplicate on 96-well optical PCR plates (Sarstedt AG, Nümbrecht, Germany) as previously described[14] using SSoFast EvaGreen SuperMix (Bio-Rad Laboratories Inc., Hercules, CA, USA) and a CFX96 Real-Time system (Bio-Rad Laboratories, Waltham, MA, USA). Transcript levels were normalized to the housekeeping gene *HPRT1*.

Statistical analysis. Mean values, S.D. and Student's *t*-test (unpaired) were calculated using Microsoft Excel (Redmont, WA, USA). A $P < 0.05$ was considered statistically significant.

Conflict of Interest

The authors declare no conflict of interest.

Acknowledgements. We thank Livio Trentin, Gianpietro Semenzato, Paolo Bernardi and Andrea Rasola for productive discussions, Doreen Cantrell and Paolo Ghia for the gift of reagents and Sonia Grassini for technical assistance. This work was supported by AIRC. The support of the MIUR (FIRB, PRIN) is also acknowledged. NC is the recipient of a FIRC fellowship.

1. Bajenoff M, Germain RN. Seeing is believing: a focus on the contribution of microscopic imaging to our understanding of immune system function. *Eur J Immunol* 2007; **37**(Suppl 1): S18–S33.
2. Kehrl JH, Hwang IY, Park C. Chemoattract receptor signaling and its role in lymphocyte motility and trafficking. *Curr Top Microbiol Immunol* 2009; **334**: 107–127.
3. Pereira JP, Kelly LM, Cyster JG. Finding the right niche: B-cell migration in the early phases of T-dependent antibody responses. *Int Immunol* 2010; **22**: 413–419.
4. Umemoto E, Hayasaka H, Bai Z, Cai L, Yonekura S, Peng X *et al.* Novel regulators of lymphocyte trafficking across high endothelial venules. *Crit Rev Immunol* 2011; **31**: 147–169.
5. Murphy PM, Baggiolini M, Charo IF, Hebert CA, Horuk R, Matsushima K *et al.* International union of pharmacology. XXII. Nomenclature for chemokine receptors. *Pharmacol Rev* 2000; **52**: 145–176.
6. Busillo JM, Benovic JL. Regulation of CXCR4 signaling. *Biochim Biophys Acta* 2007; **1768**: 952–963.
7. Kehrl JH. Chemoattractant receptor signaling and the control of lymphocyte migration. *Immunol Res* 2006; **34**: 211–227.
8. Teicher BA, Fricker SP. CXCL12 (SDF-1)/CXCR4 pathway in cancer. *Clin Cancer Res* 2010; **16**: 2927–2931.
9. Patrussi L, Baldari CT. Intracellular mediators of CXCR4-dependent signaling in T cells. *Immunol Lett* 2008; **115**: 75–82.
10. Buchner M, Baer C, Prinz G, Dierks C, Burger M, Zenz T *et al.* Spleen tyrosine kinase inhibition prevents chemokine- and integrin-mediated stromal protective effects in chronic lymphocytic leukemia. *Blood* 2010; **115**: 4497–4506.
11. Ortolano S, Hwang IY, Han SB, Kehrl JH. Roles for phosphoinositide 3-kinases, Bruton's tyrosine kinase, and Jun kinases in B lymphocyte chemotaxis and homing. *Eur J Immunol* 2006; **36**: 1285–1295.
12. Finetti F, Savino MT, Baldari CT. Positive and negative regulation of antigen receptor signaling by the Shc family of protein adapters. *Immunol Rev* 2009; **232**: 115–134.
13. Finetti F, Pellegrini M, Ulivieri C, Savino MT, Paccagnini E, Ginanneschi C *et al.* The proapoptotic and antimitogenic protein p66SHC acts as a negative regulator of lymphocyte activation and autoimmunity. *Blood* 2008; **111**: 5017–5027.
14. Capitani N, Patrussi L, Trentin L, Lucherini OM, Cannizzaro E, Migliaccio E *et al.* S1P1 expression is controlled by the pro-oxidant activity of p66Shc and is impaired in B-CLL patients with unfavorable prognosis. *Blood* 2012; **120**: 4391–4399.
15. Patrussi L, Ulivieri C, Lucherini OM, Paccani SR, Gamberucci A, Lanfrancone L *et al.* p52Shc is required for CXCR4-dependent signaling and chemotaxis in T cells. *Blood* 2007; **110**: 1730–1738.
16. Margadant C, Charafeddine RA, Sonnenberg A. Unique and redundant functions of integrins in the epidermis. *FASEB J* 2010; **24**: 4133–4152.
17. Burger JA, Zvaifler NJ, Tsukada N, Firestein GS, Kipps TJ. Fibroblast-like synoviocytes support B-cell pseudoemperipolesis via a stromal cell-derived factor-1- and CD106 (VCAM-1)-dependent mechanism. *J Clin Invest* 2001; **107**: 305–315.
18. Rougerie P, Delon J. Rho GTPases: masters of T lymphocyte migration and activation. *Immunol Lett* 2012; **142**: 1–13.
19. Swat W, Fujikawa K. The Vav family: at the crossroads of signaling pathways. *Immunol Res* 2005; **32**: 259–265.
20. Mosenden R, Tasken K. Cyclic AMP-mediated immune regulation–overview of mechanisms of action in T cells. *Cell Signal* 2011; **23**: 1009–1016.
21. Czech MP. PIP2 and PIP3: complex roles at the cell surface. *Cell* 2000; **100**: 603–606.
22. Ward SG. T lymphocytes on the move: chemokines, PI 3-kinase and beyond. *Trends Immunol* 2006; **27**: 80–87.
23. Conde C, Gloire G, Piette J. Enzymatic and non-enzymatic activities of SHIP-1 in signal transduction and cancer. *Biochem Pharmacol* 2011; **82**: 1320–1334.
24. Kim CH, Hangoc G, Cooper S, Helgason CD, Yew S, Humphries RK *et al.* Altered responsiveness to chemokines due to targeted disruption of SHIP. *J Clin Invest* 1999; **104**: 1751–1759.
25. Zhang J, Somani AK, Siminovitch KA. Roles of the SHP-1 tyrosine phosphatase in the negative regulation of cell signalling. *Semin Immunol* 2000; **12**: 361–378.
26. McLeod SJ, Shum AJ, Lee RL, Takei F, Gold MR. The Rap GTPases regulate integrin-mediated adhesion, cell spreading, actin polymerization, and Pyk2 tyrosine phosphorylation in B lymphocytes. *J Biol Chem* 2004; **279**: 12009–12019.
27. de Gorter DJ, Beuling EA, Kersseboom R, Middendorp S, van Gils JM, Hendriks RW *et al.* Bruton's tyrosine kinase and phospholipase Cgamma2 mediate chemokine-controlled B cell migration and homing. *Immunity* 2007; **26**: 93–104.
28. Durand CA, Westendorf J, Tse KW, Gold MR. The Rap GTPases mediate CXCL13- and sphingosine1-phosphate-induced chemotaxis, adhesion, and Pyk2 tyrosine phosphorylation in B lymphocytes. *Eur J Immunol* 2006; **36**: 2235–2249.
29. Durand CA, Hartvigsen K, Fogelstrand L, Kim S, Iritani S, Vanhaesebroeck B *et al.* Phosphoinositide 3-kinase p110 delta regulates natural antibody production, marginal zone and B-1 B cell function, and autoantibody responses. *J Immunol* 2009; **183**: 5673–5684.
30. Koretzky GA, Abtahian F, Silverman MA. SLP76 and SLP65: complex regulation of signalling in lymphocytes and beyond. *Nat Rev Immunol* 2006; **6**: 67–78.
31. Wange RL. LAT, the linker for activation of T cells: a bridge between T cell-specific and general signaling pathways. *Sci STKE* 2000; **2000:** re1.
32. Horn J, Wang X, Reichardt P, Stradal TE, Warnecke N, Simeoni L *et al.* Src homology 2-domain containing leukocyte-specific phosphoprotein of 76 kDa is mandatory for TCR-mediated inside-out signaling, but dispensable for CXCR4-mediated LFA-1 activation, adhesion, and migration of T cells. *J Immunol* 2009; **183**: 5756–5767.
33. Kremer KN, Humphreys TD, Kumar A, Qian NX, Hedin KE. Distinct role of ZAP-70 and Src homology 2 domain-containing leukocyte protein of 76 kDa in the prolonged activation of extracellular signal-regulated protein kinase by the stromal cell-derived factor-1 alpha/CXCL12 chemokine. *J Immunol* 2003; **171**: 360–367.
34. Smith X, Schneider H, Kohler K, Liu H, Lu Y, Rudd CE. The chemokine CXCL12 generates costimulatory signals in T cells to enhance phosphorylation and clustering of the adaptor protein SLP-76. *Sci Signal* 2013; **6**: ra65.
35. Lee D, Kim J, Baker RG, Koretzky GA, Hammer DA. SLP-76 is required for optimal CXCR4-stimulated T lymphocyte firm arrest to ICAM-1 under shear flow. *Eur J Immunol* 2012; **42**: 2736–2743.
36. Chernock RD, Cherla RP, Ganju RK. SHP2 and cbl participate in alpha-chemokine receptor CXCR4-mediated signaling pathways. *Blood* 2001; **97**: 608–615.
37. Capitani N, Lucherini OM, Sozzi E, Ferro M, Giommoni N, Finetti F *et al.* Impaired expression of p66Shc, a novel regulator of B-cell survival, in chronic lymphocytic leukemia. *Blood* 2010; **115**: 3726–3736.

38. Tabe Y, Jin L, Iwabuchi K, Wang RY, Ichikawa N, Miida T *et al.* Role of stromal microenvironment in nonpharmacological resistance of CML to imatinib through Lyn/CXCR4 interactions in lipid rafts. *Leukemia* 2012; **26**: 883–892.
39. Dustin LB, Plas DR, Wong J, Hu YT, Soto C, Chan AC *et al.* Expression of dominant-negative src-homology domain 2-containing protein tyrosine phosphatase-1 results in increased Syk tyrosine kinase activity and B cell activation. *J Immunol* 1999; **162**: 2717–2724.
40. Konigsberger S, Peckl-Schmid D, Zaborsky N, Patzak I, Kiefer F, Achatz G. HPK1 associates with SKAP-HOM to negatively regulate Rap1-mediated B-lymphocyte adhesion. *PLoS One* 2010; **5**: e12468.
41. Ulivieri C, Fanigliulo D, Masi G, Savino MT, Gamberucci A, Pelicci PG *et al.* p66Shc is a negative regulator of FcepsilonRI-dependent signaling in mast cells. *J Immunol* 2011; **186**: 5095–5106.
42. Pradhan M, Coggeshall KM. Activation-induced bi-dentate interaction of SHIP and Shc in B lymphocytes. *J Cell Biochem* 1997; **67**: 32–42.
43. Liu L, Damen JE, Hughes MR, Babic I, Jirik FR, Krystal G. The Src homology 2 (SH2) domain of SH2-containing inositol phosphatase (SHIP) is essential for tyrosine phosphorylation of SHIP, its association with Shc, and its induction of apoptosis. *J Biol Chem* 1997; **272**: 8983–8988.
44. Wu RF, Gu Y, Xu YC, Nwariaku FE, Terada LS. Vascular endothelial growth factor causes translocation of p47phox to membrane ruffles through WAVE1. *J Biol Chem* 2003; **278**: 36830–36840.
45. Ikeda S, Yamaoka-Tojo M, Hilenski L, Patrushev NA, Anwar GM, Quinn MT *et al.* IQGAP1 regulates reactive oxygen species-dependent endothelial cell migration through interacting with Nox2. *Arterioscler Thromb Vasc Biol* 2005; **25**: 2295–2300.
46. Hurd TR, DeGennaro M, Lehmann R. Redox regulation of cell migration and adhesion. *Trends Cell Biol* 2012; **22**: 107–115.
47. Lo SK, Janakidevi K, Lai L, Malik AB. Hydrogen peroxide-induced increase in endothelial adhesiveness is dependent on ICAM-1 activation. *Am J Physiol* 1993; **264**: L406–L412.
48. Takano M, Meneshian A, Sheikh E, Yamakawa Y, Wilkins KB, Hopkins EA *et al.* Rapid upregulation of endothelial P-selectin expression via reactive oxygen species generation. *Am J Physiol Heart Circ Physiol* 2002; **283**: H2054–H2061.
49. van Wetering S, van Buul JD, Quik S, Mul FP, Anthony EC, ten Klooster JP *et al.* Reactive oxygen species mediate Rac-induced loss of cell-cell adhesion in primary human endothelial cells. *J Cell Sci* 2002; **115**: 1837–1846.
50. Nemoto S, Finkel T. Redox regulation of forkhead proteins through a p66shc-dependent signaling pathway. *Science* 2002; **295**: 2450–2452.
51. Giorgio M, Migliaccio E, Orsini F, Paolucci D, Moroni M, Contursi C *et al.* Electron transfer between cytochrome c and p66Shc generates reactive oxygen species that trigger mitochondrial apoptosis. *Cell* 2005; **122**: 221–233.
52. Ushio-Fukai M. Compartmentalization of redox signaling through NADPH oxidase-derived ROS. *Antioxid Redox Signal* 2009; **11**: 1289–1299.
53. Ma Z, Myers DP, Wu RF, Nwariaku FE, Terada LS. p66Shc mediates anoikis through RhoA. *J Cell Biol* 2007; **179**: 23–31.
54. Oshikawa J, Kim SJ, Furuta E, Caliceti C, Chen GF, McKinney RD *et al.* Novel role of p66Shc in ROS-dependent VEGF signaling and angiogenesis in endothelial cells. *Am J Physiol Heart Circ Physiol* 2012; **302**: H724–H732.
55. Pacini S, Pellegrini M, Migliaccio E, Patrussi L, Ulivieri C, Ventura A *et al.* p66SHC promotes apoptosis and antagonizes mitogenic signaling in T cells. *Mol Cell Biol* 2004; **24**: 1747–1757.
56. Astoul E, Watton S, Cantrell D. The dynamics of protein kinase B regulation during B cell antigen receptor engagement. *J Cell Biol* 1999; **145**: 1511–1520.
57. Nakano T, Kodama H, Honjo T. Generation of lymphohematopoietic cells from embryonic stem cells in culture. *Science* 1994; **265**: 1098–1101.
58. Roecklein BA, Torok-Storb B. Functionally distinct human marrow stromal cell lines immortalized by transduction with the human papilloma virus E6/E7 genes. *Blood* 1995; **85**: 997–1005.
59. Migliaccio E, Giorgio M, Mele S, Pelicci G, Reboldi P, Pandolfi PP *et al.* The p66shc adaptor protein controls oxidative stress response and life span in mammals. *Nature* 1999; **402**: 309–313.
60. Finetti F, Paccani SR, Riparbelli MG, Giacomello E, Perinetti G, Pazour GJ *et al.* Intraflagellar transport is required for polarized recycling of the TCR/CD3 complex to the immune synapse. *Nat Cell Biol* 2009; **11**: 1332–1339.

Supplementary Information accompanies this paper on Cell Death and Disease website (http://www.nature.com/cddis)